20 years of splines and biomedical imaging: The prehistory

Michael Unser

Biomedical Imaging Group
EPFL, Lausanne
Switzerland

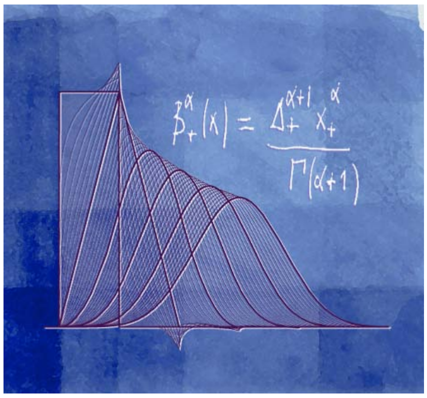

BIG's 20th Birthday, March 23, 2018, EPFL, Switzerland

Samedi 31 janvier — dimanche 1er février 1981

LAUSANNE

NOUVEAUX DIPLÔMÉS À L'EPFL

Science et conscience

Un institut interdépartemental de microélectronique, un échange avec la Carnegie Mellon University, une garderie-Chenille, le département de chimie qui prend le large du côté d'Ecublens, des manifs et des Chinois venu goûter aux vertus lémaniques, un troisième cycle en informatique technique, l'énergie solaire à la « une », un championnat de planche à voile ; et 171 nouveaux diplômés ! Bilan dressé par M. Bernard Vittoz, président de l'EPFL, lors de la cérémonie de remise des diplômes qui a eu lieu hier soir à Lausanne, en présence de nombreuses personnalités du monde politique et universitaire suisse.

« Mieux habilités à faire des nœuds routiers que des nœuds de cravate », a prétendu M. Pierre Nicod, parlant au nom des ingénieurs du génie rural de sa volée, les nouveaux diplômés ont désormais pour tâche de créer, avec les morceaux épars d'un savoir touffu, une mosaïque qui concilie la science rigoureuse et l'approche humaine, la formation reçue et celle acquise par l'expérience sur le futur terrain de leurs recherches. A cette lente transformation de jeunes étudiants en ingénieurs et architectes responsables, l'EPFL a contribué aussi largement que possible. Il appartient dès lors à chacun d'en faire l'usage que la compétence, le sens des responsabilités et la curiosité toujours en éveil lui dicteront. — (24)

M. Bernard Vittoz remet les diplômes, entouré des nombreux photographes amateurs de service !

Muriset

1981: Master in EE

1984: Ph.D. in EE

ÉCOLE POLYTECHNIQUE FÉDÉRALE DE LAUSANNE

1985-88: Visiting Fellow

1989-97: Scientist

National Institutes of health,
Biomedical Engineering and Instrumentation Program

NATIONAL INSTITUTES OF HEALTH

DEPARTMENT OF HEALTH & HUMAN SERVICES·USA

1997-2000: Associate Professor

ÉCOLE POLYTECHNIQUE FÉDÉRALE DE LAUSANNE

2000-present: Full Professor

1985-89: Electron microscopy

Volume 55 April 1989 713–724 Biophysical Journal 713

Interactions between actin and myosin filaments in skeletal muscle visualized in frozen-hydrated thin sections

B. L. Trus,* A. C. Steven,‡ A. W. McDowall,| M. Unser,§ J. Dubochet,| and R. J. Podolsky‡
*Computer Systems Laboratory, Division of Computer Research and Technology, ‡Laboratory of Physical Biology, National Institute of Arthritis, Musculoskeletal and Skin Diseases,§ Biological Engineering and Instrumentation Branch, National Institutes of Health, Bethesda, Maryland 20892; and |European Molecular Biology Laboratory, D-6900 Heidelberg, Federal Republic of Germany

ABSTRACT For the purpose of determining net interactions between actin and myosin filaments in muscle cells, perhaps the single most informative view of the myofilament lattice is its averaged axial projection. We have studied frozen-hydrated transverse thin sections with the goal of obtaining axial projections that are not subject to the limitations of conventional thin sectioning (suspect preservation of native structure) or of equatorial x-ray diffraction analysis (lack of experimental phases). In principle, good preservation of native structure may be achieved with fast freezing, followed by low-dose electron imaging of unstained vitrified cryosections. In practice, however, cryosections undergo large-scale distortions, including irreversible compression; furthermore, phase contrast imaging results in a nonlinear relationship between the projected density of the specimen and the optical density of the micrograph.

To overcome these limitations, we have devised methods of image restoration and generalized correlation averaging, and applied them to cryosections of rabbit psoas fibers in both the relaxed and rigor states. Thus visualized, myosin filaments appear thicker than actin filaments by a much smaller margin than in conventional thin sections, and particularly so for rigor muscle. This may result from a significant fraction of the myosin S1-cross-bridges averaging out in projection and thus contributing only to the baseline of projected density. Entering rigor incurs a loss of density from an annulus around the myosin filament, with a compensating accumulation of density around the actin filament. This redistribution of mass represents attachment of the fraction of cross-bridges that are visible above background. Myosin filaments in the "nonoverlap" zone appear to broaden on entering rigor, suggesting that, on deprivation of ATP, cross-bridges in situ move outwards even without actin in their immediate proximity.

Ultramicroscopy 30 (1989) 429–434
North-Holland, Amsterdam 429

SHORT NOTE

THE SPECTRAL SIGNAL-TO-NOISE RATIO RESOLUTION CRITERION: COMPUTATIONAL EFFICIENCY AND STATISTICAL PRECISION

Michael UNSER *,**
Biomedical Engineering and Instrumentation Branch, National Institutes of Health, Bethesda, Maryland 20892, USA

Benes L. TRUS
Computer Systems Laboratory, Division of Computer Research and Technology, National Institutes of Health, Bethesda, Maryland 20892, USA

Joachim FRANK
Wadsworth Center for Laboratories and Research, New York State Department of Health, Albany, New York 12201, USA

and

Alasdair C. STEVEN
Laboratory of Physical Biology, National Institute of Arthritis, Musculoskeletal and Skin Diseases, National Institutes of Health, Bethesda, Maryland 20892, USA

Received 14 March 1989

This note describes a practical improvement in the computational efficiency of the spectral signal-to-noise ratio (SSNR) resolution criterion for correlation-averaged images. The total set of N images is randomly partitioned into n_g subsets, each subset is separately averaged, and a reduced form of the SSNR is computed from these average images. In general, larger values of n_g achieve lower statistical uncertainty, while smaller values of n_g are computationally more expedient. It is shown that, for negatively stained data, a judicious compromise is achieved with $10 \leq n_g \leq 20$, regardless of how large N may be.

Jacques Dubochet, Joachim Frank, Richard Henderson

Nobel Prize in Chemistry 2017

"for developing cryo-electron microscopy for the high-resolution structure determination of biomolecules in solution"

1990-93: Splines and signal processing

IEEE TRANSACTIONS ON PATTERN ANALYSIS AND MACHINE INTELLIGENCE, VOL. 13, NO. 3, MARCH 1991

Fast B-Spline Transforms for Continuous Image Representation and Interpolation

Michael Unser, Akram Aldroubi, and Murray Eden

***Abstract*—This correspondence describes efficient algorithms for the continuous representation of a discrete signal in terms of B-splines (direct B-spline transform), and for interpolative signal reconstruction (indirect B-spline transform) with an expansion factor *m*. Expressions for the *z*-transforms of the sampled B-spline functions are determined and a convolution property of these kernels is established. It is shown that both the direct and indirect spline transforms involve linear operators that are**

Manuscript received June 14, 1989; revised July 19, 1990. Recommended for acceptance by R. J. Woodham.

M. Unser is with the Biomedical Engineering and Instrumentation Program, National Institutes of Health, Bethesda, MD 20892, and INSERM, Unité 2, Hôpital Henri-Mondor, F-94010 Créteil, France.

A. Aldroubi and M. Eden are with the Biomedical and Instrumentation Program, National Institutes of Health, Bethesda, MD 20892.

IEEE Log Number 9040953.

IEEE TRANSACTIONS ON SIGNAL PROCESSING, VOL. 41, NO. 2, FEBRUARY 1993 821

B-Spline Signal Processing: Part I—Theory

Michael Unser, *Member, IEEE*, Akram Aldroubi, and Murray Eden, *Life Fellow, IEEE*

***Abstract*—This paper describes a set of efficient filtering techniques for the processing and representation of signals in terms of continuous B-spline basis functions. We first consider the problem of determining the spline coefficients for an exact signal interpolation (direct B-spline transform). The reverse operation is the signal reconstruction from its spline coefficients with an optional zooming factor *m* (indirect B-spline transform). We derive general expressions for the *z* transforms and the equivalent continuous impulse responses of B-spline interpolators of order *n*. We present simple techniques for signal differentiation and filtering in the transformed domain. We then derive recursive filters that efficiently solve the problems of smoothing spline and least squares approximations. The smoothing spline technique approximates a signal with a complete set of coefficients subject to certain regularization or smoothness constraints. The least squares approach, on the other hand, uses a reduced number of B-spline coefficients with equally spaced nodes; this technique is in many ways analogous to the application of antialiasing low-pass filter prior to decimation in order to represent a signal correctly with a reduced number of samples.**

Edge detection is a good example in which the use of a continuous signal representation is particularly apposite. Most algorithms are based on the evaluation of spatial gradients or Laplacians [5]. Early techniques relied on finite differences to estimate these quantities [6], [7]; however, these simple operators used on noisy images perform poorly. More recent approaches often depend on the concept of fitting a continuous surface locally to the data [5], [8], [9]. Haralick used local least squares polynomial fits to determine the zero crossing of the directional second derivatives [9]. Poggio *et al.* proposed a smoothing cubic spline technique to improve the estimation of the intensity gradient in the presence of noise [10], [11]. These authors showed the approach to be more or less equivalent to smoothing the image with a Gaussian low-pass filter in a preprocessing step. In fact, an initial smoothing operation is implicit to all least squares techniques and is used in almost any modern edge detection

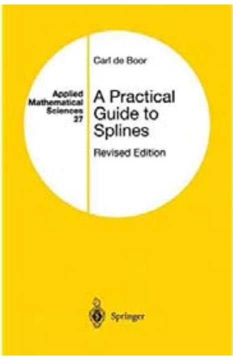

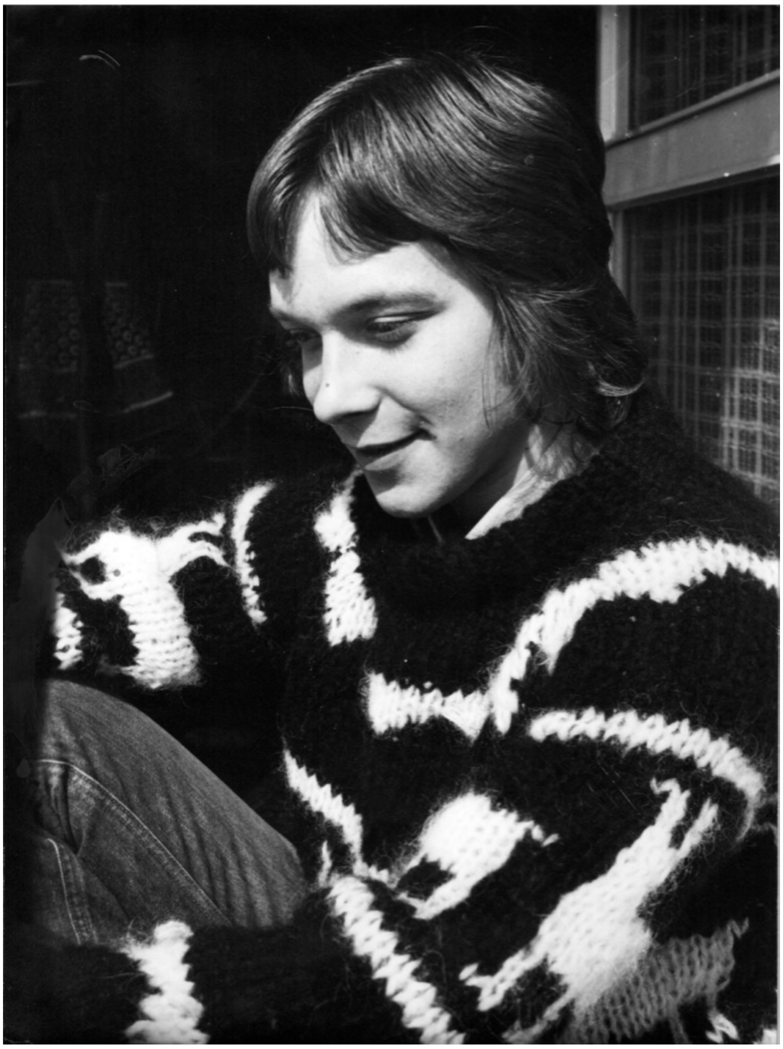

1991-93: Splines and wavelets

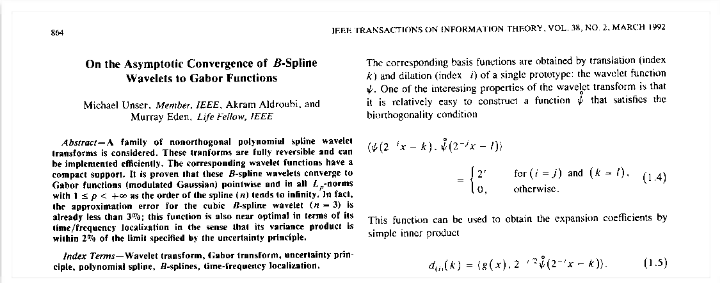

864 IEEE TRANSACTIONS ON INFORMATION THEORY, VOL. 38, NO. 2, MARCH 1992

On the Asymptotic Convergence of *B*-Spline Wavelets to Gabor Functions

Michael Unser, *Member, IEEE*, Akram Aldroubi, and Murray Eden, *Life Fellow, IEEE*

***Abstract*—A family of nonorthogonal polynomial spline wavelet transforms is considered. These tranforms are fully reversible and can be implemented efficiently. The corresponding wavelet functions have a compact support. It is proven that these *B*-spline wavelets converge to Gabor functions (modulated Gaussian) pointwise and in all L_p-norms with $1 \le p < +\infty$ as the order of the spline (n) tends to infinity. In fact, the approximation error for the cubic *B*-spline wavelet ($n = 3$) is already less than 3%; this function is also near optimal in terms of its time/frequency localization in the sense that its variance product is within 2% of the limit specified by the uncertainty principle.**

***Index Terms*—Wavelet transform, Gabor transform, uncertainty principle, polynomial spline, *B*-splines, time-frequency localization.**

The corresponding basis functions are obtained by translation (index k) and dilation (index i) of a single prototype: the wavelet function ψ. One of the interesting properties of the wavelet transform is that it is relatively easy to construct a function $\mathring{\psi}$ that satisfies the biorthogonality condition

$$\langle \psi(2^{-i}x - k), \mathring{\psi}(2^{-j}x - l) \rangle = \begin{cases} 2^{i} & \text{for } (i = j) \text{ and } (k = l), \\ 0, & \text{otherwise.} \end{cases} \quad (1.4)$$

This function can be used to obtain the expansion coefficients by simple inner product

$$d_{(i)}(k) = \langle g(x), 2^{-i/2}\mathring{\psi}(2^{-i}x - k) \rangle. \quad (1.5)$$

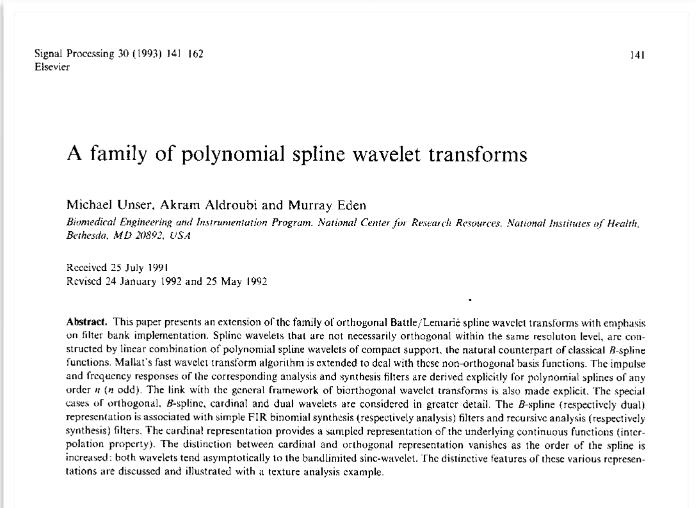

Signal Processing 30 (1993) 141 162
Elsevier

141

A family of polynomial spline wavelet transforms

Michael Unser, Akram Aldroubi and Murray Eden
Biomedical Engineering and Instrumentation Program, National Center for Research Resources, National Institutes of Health, Bethesda, MD 20892, USA

Received 25 July 1991
Revised 24 January 1992 and 25 May 1992

Abstract. This paper presents an extension of the family of orthogonal Battle/Lemarié spline wavelet transforms with emphasis on filter bank implementation. Spline wavelets that are not necessarily orthogonal within the same resoluton level, are constructed by linear combination of polynomial spline wavelets of compact support, the natural counterpart of classical *B*-spline functions. Mallat's fast wavelet transform algorithm is extended to deal with these non-orthogonal basis functions. The impulse and frequency responses of the corresponding analysis and synthesis filters are derived explicitly for polynomial splines of any order n (n odd). The link with the general framework of biorthogonal wavelet transforms is also made explicit. The special cases of orthogonal, *B*-spline, cardinal and dual wavelets are considered in greater detail. The *B*-spline (respectively dual) representation is associated with simple FIR binomial synthesis (respectively analysis) filters and recursive analysis (respectively synthesis) filters. The cardinal representation provides a sampled representation of the underlying continuous functions (interpolation property). The distinction between cardinal and orthogonal representation vanishes as the order of the spline is increased; both wavelets tend asymptotically to the bandlimited sinc-wavelet. The distinctive features of these various representations are discussed and illustrated with a texture analysis example.

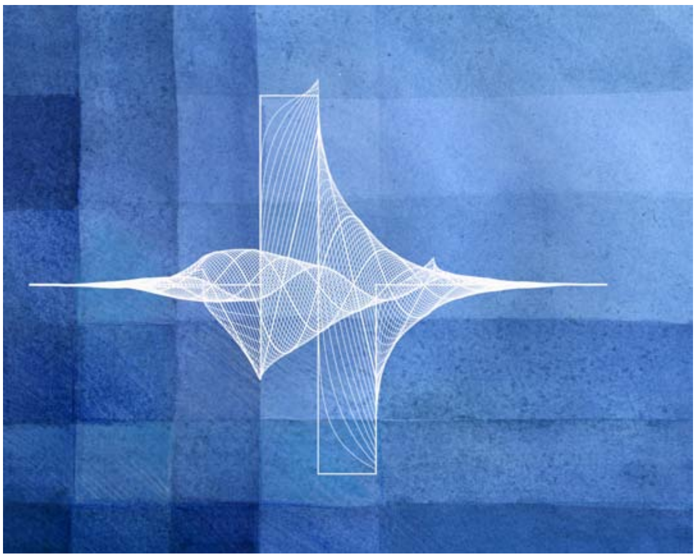


Lumini 2009

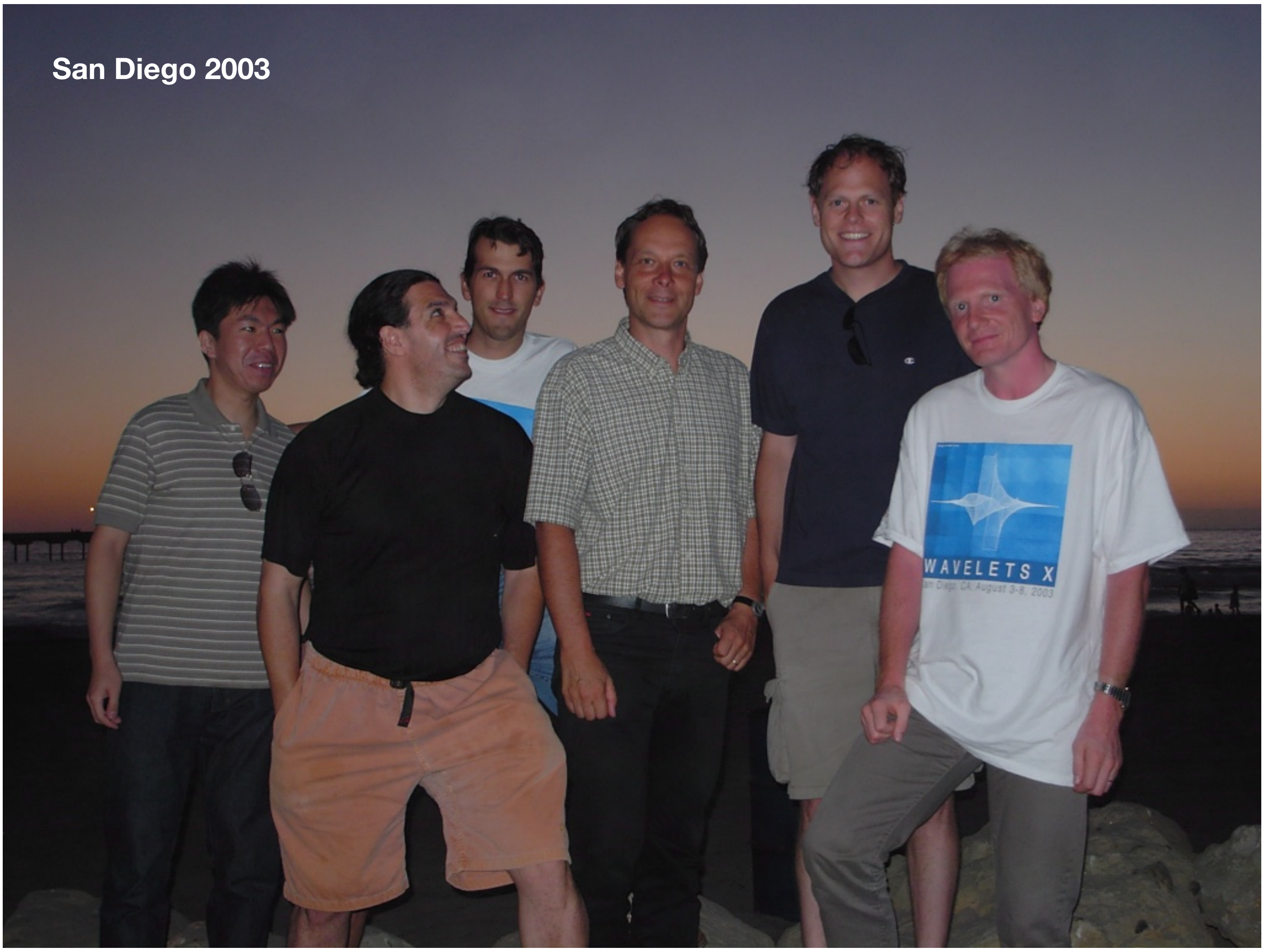

San Diego 2003

1991-97: Wavelets in medicine and biology

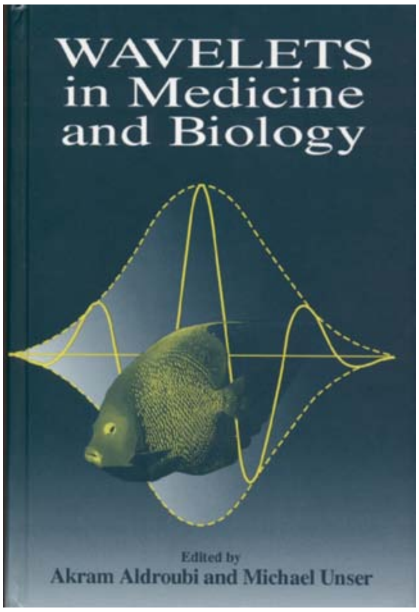

CRC Press, 1996

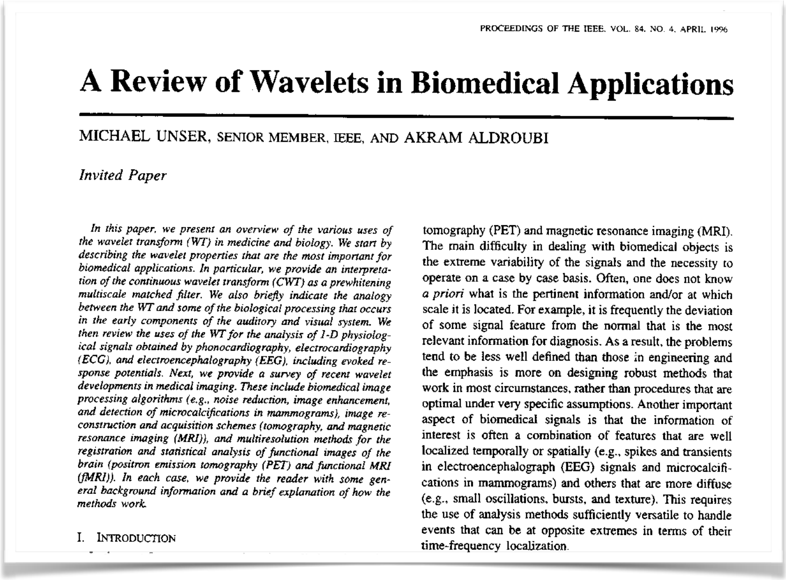

PROCEEDINGS OF THE IEEE, VOL. 84, NO. 4, APRIL 1996

A Review of Wavelets in Biomedical Applications

MICHAEL UNSER, SENIOR MEMBER, IEEE, AND AKRAM ALDROUBI

Invited Paper

In this paper, we present an overview of the various uses of the wavelet transform (WT) in medicine and biology. We start by describing the wavelet properties that are the most important for biomedical applications. In particular, we provide an interpretation of the continuous wavelet transform (CWT) as a prewhitening multiscale matched filter. We also briefly indicate the analogy between the WT and some of the biological processing that occurs in the early components of the auditory and visual system. We then review the uses of the WT for the analysis of 1-D physiological signals obtained by phonocardiography, electrocardiography (ECG), and electroencephalography (EEG), including evoked response potentials. Next, we provide a survey of recent wavelet developments in medical imaging. These include biomedical image processing algorithms (e.g., noise reduction, image enhancement, and detection of microcalcifications in mammograms), image reconstruction and acquisition schemes (tomography, and magnetic resonance imaging (MRI)), and multiresolution methods for the registration and statistical analysis of functional images of the brain (positron emission tomography (PET) and functional MRI (fMRI)). In each case, we provide the reader with some general background information and a brief explanation of how the methods work.

I. Introduction

tomography (PET) and magnetic resonance imaging (MRI). The main difficulty in dealing with biomedical objects is the extreme variability of the signals and the necessity to operate on a case by case basis. Often, one does not know *a priori* what is the pertinent information and/or at which scale it is located. For example, it is frequently the deviation of some signal feature from the normal that is the most relevant information for diagnosis. As a result, the problems tend to be less well defined than those in engineering and the emphasis is more on designing robust methods that work in most circumstances, rather than procedures that are optimal under very specific assumptions. Another important aspect of biomedical signals is that the information of interest is often a combination of features that are well localized temporally or spatially (e.g., spikes and transients in electroencephalograph (EEG) signals and microcalcifications in mammograms) and others that are more diffuse (e.g., small oscillations, bursts, and texture). This requires the use of analysis methods sufficiently versatile to handle events that can be at opposite extremes in terms of their time-frequency localization.

BIG’s research agenda

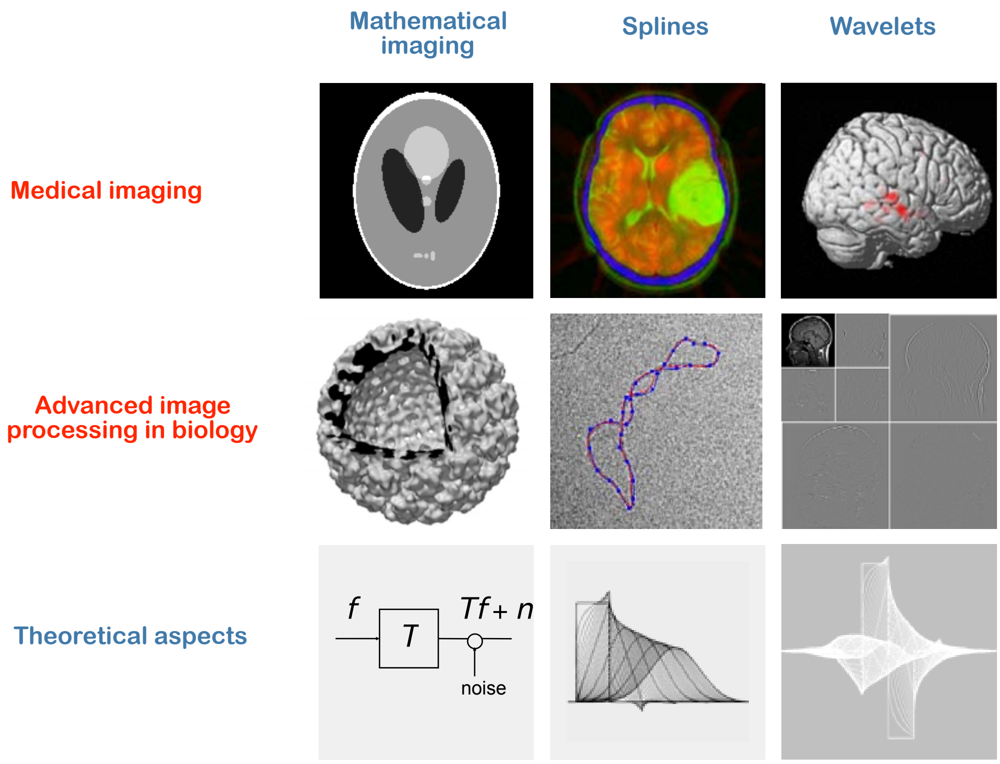

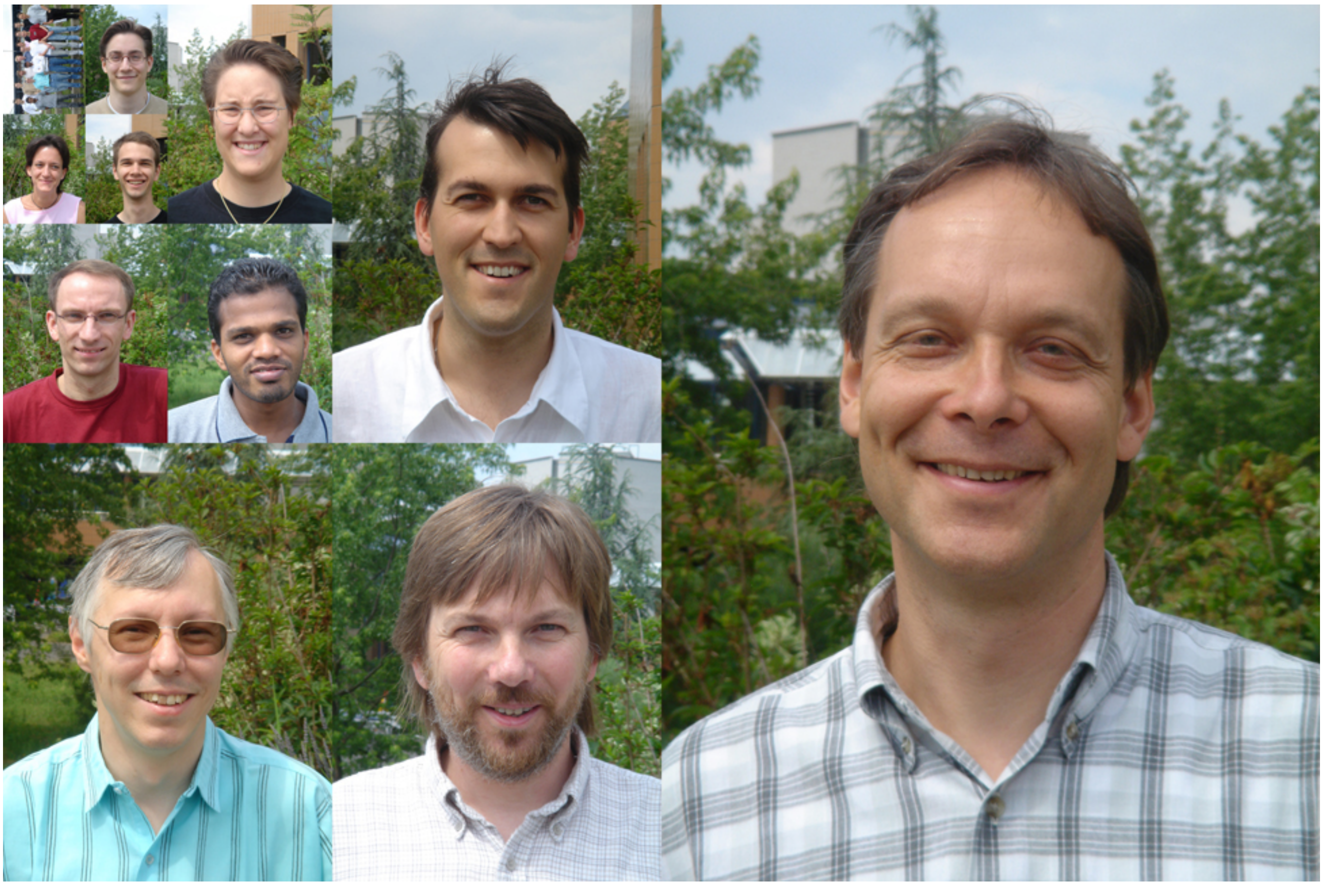

One BIG Memory: going fractional

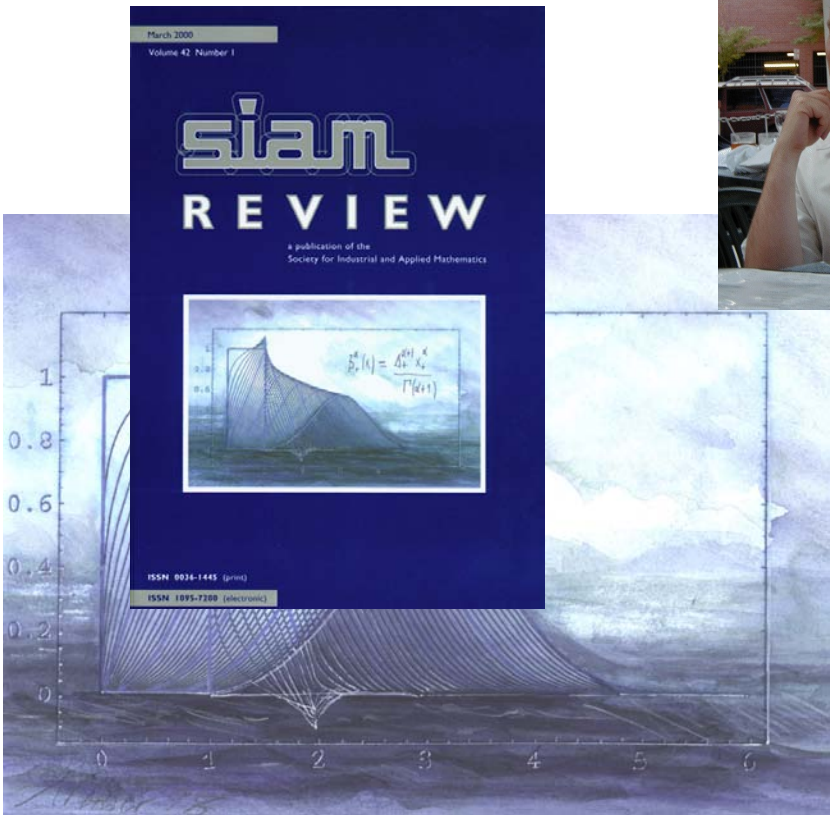

IEEE Signal Processing Magazine

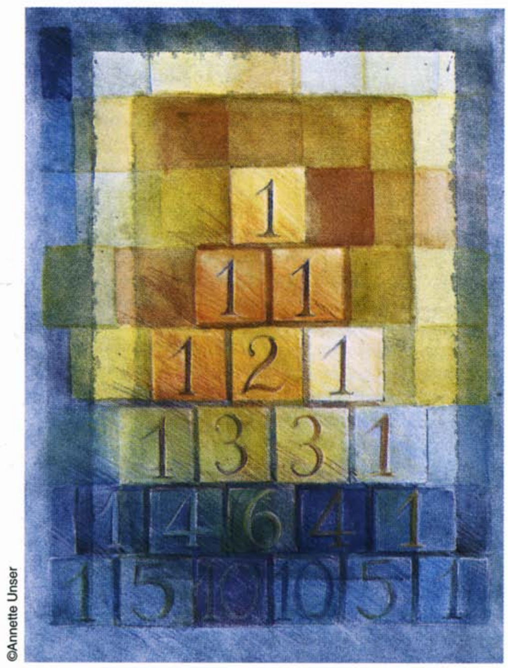

Splines

A Perfect Fit for a scientific career

June 2028++